DOI: 10.1002/ejic.200801218

A Chloro-Bridged Linear Chain Imine-Copper(II) Complex and Its Application as an Enzyme-Free Amperometric Biosensor for Hydrogen Peroxide

Wendel A. Alves,*[a] Iorquirene O. Matos,[a] Pedro M. Takahashi,[a] Erick L. Bastos,[a] Herculano Martinho,[a] Janaina G. Ferreira,[b,c] Claudia C. Silva,[b,d] Regina H. de Almeida Santos,[b] Armando Paduan-Filho,[e] and Ana M. Da Costa Ferreira*[f]

Keywords: Sensors / Enzyme-free biosensors / Hydrogen peroxide detection / Copper(II) complexes / Structural characterization / Magnetic properties

The synthesis, structural characterisation and magnetic properties of a new chloro-bridged linear chain imine-copper(II) compound are reported. The results indicate that uniform chains are formed by stacking of parallel pyramidal units formed from the copper centre coordinated to the imine ligands and bridged by chloride ions, with the uncoordinated perchlorate ions located between the layers to balance the charge. Magnetic measurements carried out on a powder sample at temperatures from 1.8 to 290 K and a field of 500 Oe, indicated an intramolecular magnetic coupling between the copper centres [J/k = (–12.3 ± 0.2) K]. Moreover, an antiferromagnetic interaction can also be observed between the polynuclear arrays [$J'z/k$ = –(10.4 ± 1.7) K]. An analysis of the sample at high temperature indicated that the overall interaction would be antiferromagnetic (Θ_{CW} = –14 K). Furthermore, this new inorganic-organic zigzag polymer was linked covalently to the poly(*N*-vinylimidazole) polymer, PVI, on a vitreous carbon electrode surface and used as a biomimetic material for the efficient analytical determination of hydrogen peroxide. Raman spectroscopy and electrochemical techniques were used to give a complete characterisation of the hybrid film obtained. The proposed enzyme-free biosensor for catalase-like activity exhibited good sensitivity (268 mA mol^{-1} L cm^{-2}) at –0.4 V relative to the. SCE in a phosphate buffer solution (pH 7.0) and a wide linear range from 1 to 30 mmol L^{-1} for hydrogen peroxide detection.

Introduction

In recent years molecular electronics research has generated considerable interest.[1] New metallopolymers have been synthesised for creating molecular devices.[2] In particular, electrodes modified with polymer-based films containing charge carriers (e.g. redox mediators attached to a polymer backbone) and enzymes (e.g. glucose and bilirubin oxidases) dispersed into a matrix are of technological importance in the design of novel electrochemical sensors for analytical applications and in providing improved electrodes for biofuel cells.[3] Enzyme-modified electrodes have been extensively explored and enzymes are used in many chemical processes.[4] However, in spite of showing outstanding activity as well as high specificity and selectivity, they have the drawback of working at near physiological conditions and are often expensive and unstable during extended usage although their active lifetimes can be extended by immobilisation on electrode surfaces by means of entrapment, chemical bonding and crosslinking.[5] These limitations have, therefore, led to extensive efforts on developing syntheses of *enzyme-free biosensors* with a centre resembling the 3D catalytic active site of the enzymes.[6]

Catalase, one of the three major sensitive protective enzymes in living organisms, exists in almost all aerobically respiring organisms. It protects cells from the toxic effects of hydrogen peroxide (H_2O_2), the latter being linked to a variety of pathological consequences such as aging, diabetes and cancer.[7] Therefore, detection of hydrogen peroxide has received tremendous attention in sensor research for decades. So far, many techniques have been used from chemical, biological, clinical and environmental, and many other impressive applications have been developed.[8] Among

[a] Centro de Ciências Naturais e Humanas, Universidade Federal do ABC,
Rua Santa Adélia 166, 09210-170 Santo André, SP, Brazil
Fax: +55-11-4996-3166
E-mail: wendel.alves@ufabc.edu.br
[b] Instituto de Química de São Carlos, Universidade de São Paulo,
São Carlos, SP, Brazil
[c] Instituto de Química, UNESP,
14801-970 Araraquara, SP, Brazil
[d] Universidade do Estado do Amazonas,
69065-020 Manaus, AM, Brazil
[e] Instituto de Física, Universidade de São Paulo,
São Paulo, SP, Brazil
[f] Instituto de Química, Universidade de São Paulo,
C. P. 26077, 05513-970 São Paulo, SP, Brazil
Fax: +55-11-3815-5579
E-mail: amdcferr@iq.usp.br

Supporting information for this article is available on the WWW under http://www.eurjic.org or from the author.

them, amperometric detection is one of the most promising approaches for achieving accurate, separate and rapid H_2O_2 monitoring.[9] In recent years, enzyme-based (e.g. peroxidase and cytochrome *c*) electrodes have been developed for H_2O_2 detection with simplicity, high sensitivity and selectivity.[10] However, their operational conditions are generally limited by the denaturation of enzymes. Prussian blue (PB) and its analogues have been explored in a variety of H_2O_2 determination assays.[11] Recently, supramolecular complex dentrimers-PB membranes and silver-DNA hybrid films have been developed as catalytic layers for detecting H_2O_2.[12] Despite these advances, it is still a great challenge to construct highly selective, sensitive and stable biorecognition interfaces for the determination of H_2O_2.

The molecular self-assembly of coordination polymers is a potential route to novel 1-, 2- and 3D networks for applications in amperometric sensor devices.[2e,4b] The preparation of polymeric complexes can be accomplished by using rationally designed polydentate ligands.[13] These have received considerable attention because of their potential applications in the fields of catalysis, separation, gas storage, molecular magnetic materials and host-guest chemistry.[13,14] Porous coordination polymers are particularly attractive synthetic goals for catalysis because they have the potential to uphold reactive species, such as transition metals, along pore walls.[13–15] Indeed, they could provide new functional materials with a switching ability and in more specific cases the ability to sequester/release guest molecules or ions according to the delivered external information.

An enormous number and variety of discrete, isolable, supramolecular coordination chemistry-based assemblies featuring well-defined nanoscale cavities have been designed, synthesised and characterised over the past decade.[13–15] Among them, copper(II) complexes with imine ligands containing imidazolate-bridging groups have been investigated, leading to highly ordered, symmetrical molecular or supramolecular structures.[16] Recently, we have reported the synthesis and characterisation of some new copper(II) complexes containing an imidazolate group incorporated in the imine ligand as precursors to dinuclear and polynuclear species, the latter being designed to act as active species for the homogeneous catalysis of phenol or catechol oxidation.[17] Moreover, one of these precursor complexes was immobilised into hexaniobate nanoscrolls by an ion exchange reaction and its reactivity was investigated for catechol oxidation in the presence of hydrogen peroxide.[18] However, fairly few examples of infinite 1D molecular zigzag polymeric chains based on this type of ligand have been reported so far.

In this work, we describe the synthesis, structural characterisation and magnetic properties of a new linear chain chloride-bridged imine-copper(II) compound (see Figure 1). Furthermore, the new inorganic-organic zigzag polymer reported here was linked covalently to the PVI polymer, on a vitreous carbon electrode surface and used as a biomimetic material for the analytical determination of hydrogen peroxide. To the best of our knowledge, this is the first time that a disposable polymer of an imine-copper(II) complex has been employed in the development of an amperometric sensor for the analytical determination of hydrogen peroxide.

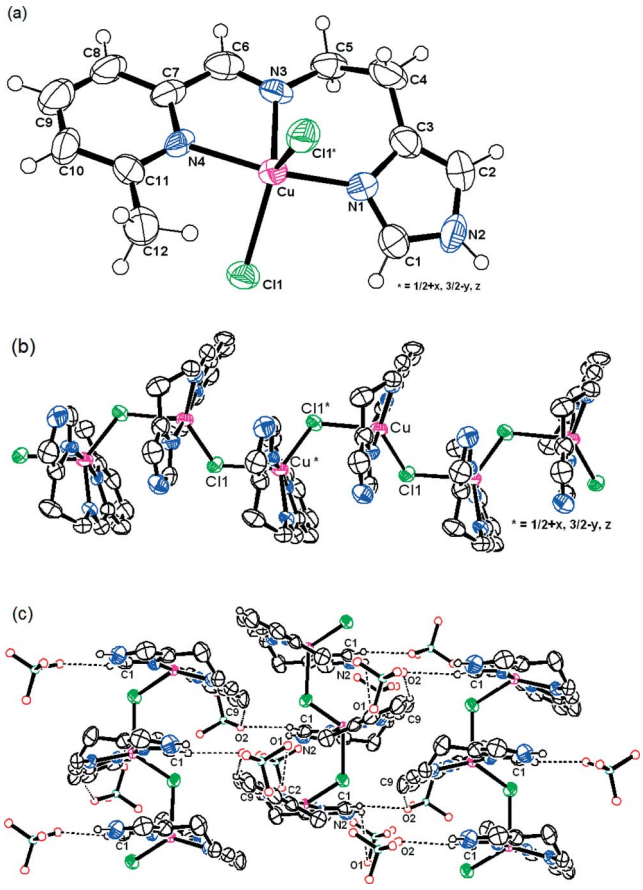

Figure 1. (a). Perspective view of the crystallographically independent $[Cu(2pymehist)Cl]^+$ monomeric unit with the atom labelling. Thermal ellipsoids are plotted at the 50% of probability level and the hydrogen atoms have been given arbitrary radii; (b) ORTEP representation of the 1D zigzag architecture in the cationic parts of the coordination polymers. All hydrogen atoms are omitted for clarity; (c) 3D network for the compound $[Cu(2pymehist)Cl](ClO_4)$, in the solid state, as determined by X-ray crystallography. The polymeric chains are shown at the 50% probability level and the perchlorate ion with arbitrary size. All hydrogen atoms except those involved in hydrogen bonding have been omitted for clarity.

Results and Discussion

The metallation of the tridentate imine ligand 2-(4-imidazolyl)-ethylimino-6-methylpyridine with copper(II) perchlorate, in acid solution, led to the chloride-bridged polynuclear complex $[Cu(2pymehist)Cl](ClO_4)$. Elemental analysis results were consistent with the proposed formula, the latter also being corroborated by conductivity measurements as shown in the experimental section. The prepared complex was additionally characterised by spectroscopic and magnetic techniques and its molecular structure determined from single-crystal X-ray diffraction data. The corresponding mononuclear $[Cu(2pymehist)Cl_2]$ species has al-

ready been characterised by Matsumoto and co-workers by X-ray diffraction.[19] Herein, we focused on the influence of the counterion on the structural features, since a 1D linear chain compound was obtained in the presence of perchlorate instead of chloride salts. When the same reaction was carried out with copper(II) chloride as the precursor material, the chloride ligands remained bonded to the copper(II) ion, saturating the coordination positions and a mononuclear complex was obtained.[19] A similar equilibrium has been studied by our group for dinuclear copper(II) complexes with a tridentate imine ligand, *apyambi* [or 2-(benzimidazolyl)methylene-2-amino-1-ethylpyridine], containing chloro-bridges such as perchlorate, nitrate or chloride salts and characterised by different techniques.[20]

Structural and Spectroscopic Characterisation of [Cu(2pymehist)Cl](ClO4)

The molecular structure of [Cu(2pymehist)Cl](ClO_4) was obtained from single-crystal X-ray diffraction data. The structure is comprised of the Cu compound, one perchlorate anion and 0.33 waters of crystallisation per unit. Selected bond lengths and angles are listed in Tables S1 and S2 in the Supporting Information and the ORTEP views are given in Figure 1. The coordination around the copper atom is a distorted tetragonal pyramidal environment generated from three nitrogen atoms from the 2pymehist ligand and two chloro-bridging ligands coordinated to each Cu^{II} ion, as certified by Reedijk's τ factor of 0.2 (τ = 0 for a square pyramid, and τ = 1 for a trigonal bipyramid).[21] The copper ion is displaced by 0.402(3) Å from the mean basal plane towards the apical Cl atom.

The structure of the mono-μ-chloro-bridged copper(II) compound may be visualised as uniform chains formed by stacking of parallel pyramidal units. The uncoordinated perchlorate ions are located between the layers in order to balance the charge. In this compound, the two Cu–Cl bond lengths are very different from each other [2.322(2) and 2.614(2) Å] but comparable with the Cu–Cl bond lengths found for Cu(ImH)Cl_2 (ImH = imidazole) in which one chlorine atom forms a bridge between successive symmetry-related copper atoms and a polynuclear chain is formed with alternating short and long Cu–Cl distances of 2.365 and 2.751 Å, respectively.[22] For the chlorine atom, which occupies a position in the basal plane of the copper ion, this distance of 2.321(2) Å is close to the sum of the covalent radii for copper and chlorine (2.27 Å) given by Pauling.[23] The Cu–Cl bond length of 2.614(2) Å observed at the fifth coordination site is comparable with the sum of the ionic radii ($r_{Cu^{2+}}$ = 0.81 Å and r_{Cl^-} = 1.81 Å) of 2.62 Å. The Cu···Cu distance in the [Cu(2pymehist)Cl](ClO_4) core is 4.234(5) Å and the Cu–Cl–Cu angle is 118.03(7)° which falls in the normal range.[24] The average Cu–N bond length is 1.999(6) Å and in the organic ligand, the N–C and C–C bond lengths in the pyridine and imidazole groups are in the expected ranges. The crystal packing reveals that the cations of the 1D polymeric chains are engaged in C–H···O hydrogen-bonding interactions by means of the imine ligand and ClO_4^- counterions, affording a 3D supramolecular network which is illustrated in Figure 1 (c) (see Table S3 in the Supporting Information).

The electronic spectrum of this copper(II) complex recorded in methanol solution exhibits two intense bands at 203 nm ($\varepsilon = 22\times10^3\ mol^{-1}\,L\,cm^{-1}$) and 299 nm ($\varepsilon = 8\times10^3\ mol^{-1}\,L\,cm^{-1}$) attributed to internal ligand transitions, as well as an asymmetric characteristic copper d-d band at 744 nm ($\varepsilon = 135\ mol^{-1}\,L\,cm^{-1}$) indicative of a pyramidal geometry as seen in the crystal geometry. Presumably all four d–d transitions $^2A[(d_{x^2-y^2})^1]\rightarrow{}^2A[(d_{z^2})^1]$, $^2A[(d_{xy})^1]$, $^2A[(d_{xz})^1]$, $^2A[(d_{yz})^1]$ expected for a square-pyramidal geometry are responsible for this band.[25] Likewise, the spectrum also shows a strong absorption at 350 nm that can be assigned to the Cl→Cu charge-transfer transition (data not shown).

The X-band EPR spectra of the polycrystalline powder [Cu(2pymehist)Cl](ClO_4) at different temperatures show a broad isotropic copper(II) signal centred around a g value of 2.06. The EPR spectrum at 126 K showed a narrowing of the line and better resolution of the hyperfine structure [see Figure 2 (a) which is characteristic of axial symmetry with $g_\perp$ = 2.116 and $g_\parallel$ = 2.483]. This narrowing probably comes from an electronic exchange between the paramagnetic centres which has the effect of averaging interactions, such as hyperfine and magnetic dipole, something which usually leads to line broadening but that can also lead to a narrowing of the lines as observed in this work.[26]

The EPR spectra of this polynuclear complex in frozen methanol exhibit a resolved hyperfine structure in the $g_\parallel$ region, around 3100 G, with some detectable lines as shown in Figure 2 (b, black line), with $g_\perp$ = 2.055 and $g_\parallel$ = 2.223. This feature arises from the overlap of two sets of peaks, corresponding to two different copper(II) complexes in tetragonal environments, probably due to the equilibrium between the polynuclear μ-chloro bridged species [Cu(2pymehist)Cl](ClO_4) and the related mononuclear aqua-compound $[Cu(2pymehist)(H_2O)_2]^{2+}$. Furthermore, EPR spectra obtained in a frozen methanol/water (4:1, v/v) mixture corroborate this mono-/polynuclear species equilibrium, as shown in Figure 2 (b) (red line, mononuclear species spectrum). In aqueous solution the mononuclear complex $[Cu(2pymehist)(H_2O)_2]^{2+}$ is predominantly formed while in methanol both species can be observed in equal quantities as a result of μ-chloro-bridges dissociation. Likewise, a weak absorption corresponding to the ΔM_s = 2 forbidden transition can be observed at "half-field" values (ca. 1500 G). This signal is characteristic of the presence of interactions between two copper(II) ions to give a triplet state. An attempt to calculate the distance between these copper ions, from the relative intensities of both signals,[27] was not successful because of the partial overlapping of the mean signal with the ΔM_s = 2. Moreover, the complex showed a superhyperfine multiplet structure due to ^{14}N atoms around the copper ion in the $g_\perp$ region when dissolved in methanol. This multiplet showed seven lines with $A_{N\perp}$ = 14.0 G as expected for at least three ^{14}N atoms

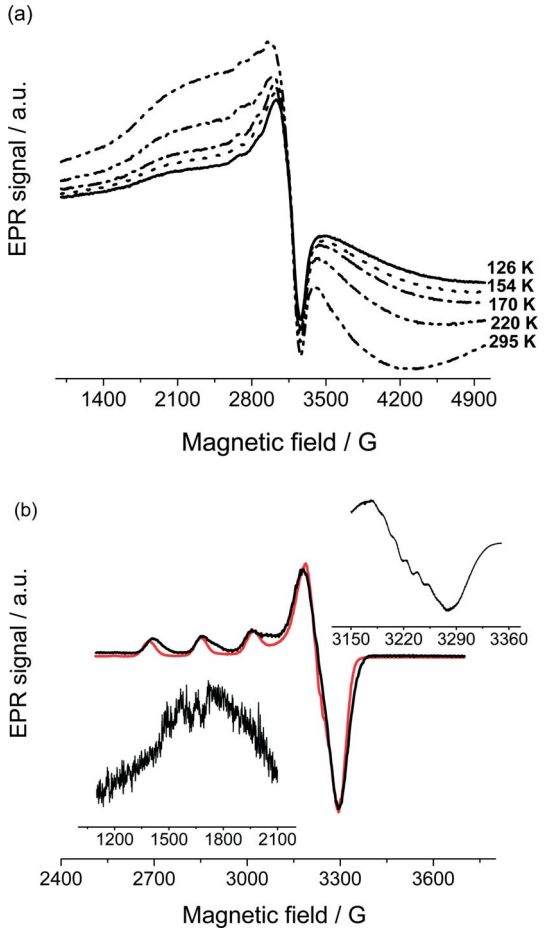

Figure 2. EPR spectra of the [Cu(2pymehist)Cl](ClO$_4$) complex in solid state at different temperatures (a) and in frozen methanol solution (black line) and methanol/water (4:1, v/v) mixture (red line), indicating an equilibrium between the mono- and the corresponding polynuclear species (b).

strongly coordinated to copper, in an approximately tetragonal ligand field, as shown in Figure 2 (b).[28]

Magnetic Properties and Magneto-Structural Correlations

A study of magnetic susceptibility data for the complex [Cu(2pymehist)Cl](ClO$_4$) within the temperature range 1.8–290 K at field of 500 Oe on a powder sample has been performed. In Figure 3 (a), the magnetic susceptibilities, χ (left scale), and their reciprocals, χ^{-1} (right scale) are shown. The magnetic susceptibility measured shows a maximum around 10 to 15 K, indicating an antiferromagnetic 1D Heisenberg chain.[27c] In the strictly paramagnetic regime at high temperatures it is expected that the system should behave according to the Curie–Weiss (CW) expression. For $T > 30$ K, χ indeed exhibited CW behaviour and fitting the data to the expression (dashed line)

$$\chi^{-1} = (T - \Theta_{CW})/C$$

furnished $\Theta_{CW} = -14$ K and $C = 0.438$ K emu^{-1}. The negative sign of Θ_{CW} indicates antiferromagnetic correlations between Cu^{II} ions.

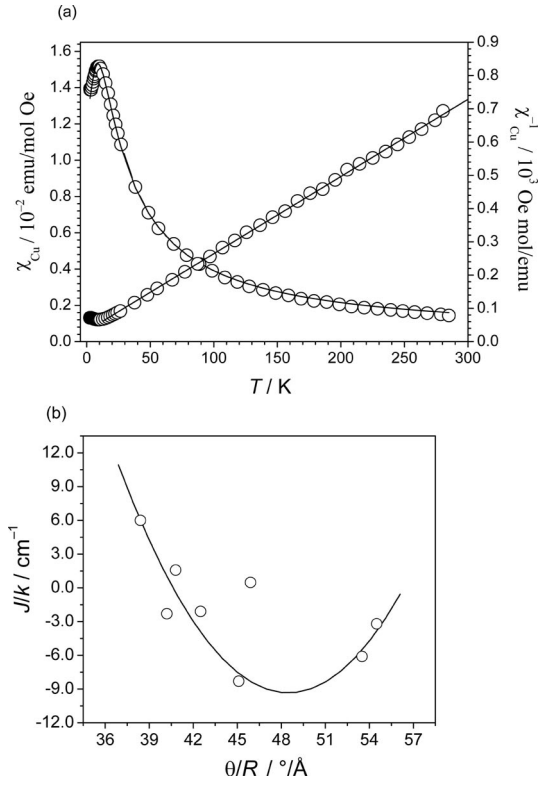

Figure 3. Temperature dependence of the magnetic susceptibility, χ_{Cu}, for the polynuclear compound [Cu(2pymehist)Cl](ClO$_4$) in the range 1.80–290 K (a); Plot of the singlet-triplet splitting J/k as a function of θ/R, in different polynuclear copper complexes (b).

The Heisenberg Hamiltonian for this system with an exchange interaction between pairs of Cu^{II} ions, with spins S_i and S_j is of the form:[27c,29]

$$H = \Sigma_{i>j} H_{ij} = \Sigma_{i>j} -2J_{ij}S_iS_j$$

in which we assume interactions between nearest neighbouring copper ions on a chain (i.e., $J_{ij} = J$ for $j = i \pm 1$ and $J_{ij} = 0$ otherwise). The detailed analysis of data was based on the Bonner and Fisher model for a 1D infinite-chain structure for which $J/k < 0$[30] but assuming a first-order molecular field correction to account for interchain interactions ($J' z/k$).[31] In this case the effective field in the sample is $H_{eff} = H + \gamma M$. H is the external applied field where $\gamma = 2J' z/Ng^2\mu_B{}^2$ and z is the number of nearest neighbouring chains interacting through the exchange J'. The corrected susceptibility actually measured is then:

$$\chi = Ng^2\mu_B{}^2 S(S + 1)/3kT \{(1 - u)/(1 + u)\} \quad (1)$$

where $u = (T/T_0) - \coth(T_0/T)$ and $T_0 = 2JS(S + 1)/k$

$$\chi' = M/H_{eff} = M/(H + \gamma M), \text{ or } \chi' = \chi/(1 - \gamma\chi) \quad (2)$$

With the substitution of Equation (1) into (2), we get (3):

$$\chi_{Cu} = \{0.0937(A/T)[1 - 0.67(T/B) + \cosh(1.5(B/T))/\sinh(1.5(B/T))]/[1 + 0.67(T/B) - \cosh(1.5(B/T))/\sinh(1.5(B/T))]\}/\{1 + C[0.0937(A/T)[1 - 0.67(T/B) + \cosh(1.5(B/T))/\sinh(1.5(B/T))]/[1 + 0.67(T/B) - \cosh(1.5(B/T))/\sinh(1.5(B/T))]]\} \quad (3)$$

where $A = S(S + 1)$; $B = J/k$; and $C = J' z/k$

The experimental data presented in Figure 3 (a) were fitted to Equation (3) by considering the g value to be fixed to that observed by EPR but with J/k and $J'z/k$ being allowed to vary freely. The best-fit values were J/k = (–12.3 ± 0.2) K, $J'z/k$ = (–10.4 ± 1.7) K and S = 1.63 (solid line in right scale of Figure 3, a).These results indicate intra- and interchain antiferromagnetic interactions with $J < 0$. The value of J is small as expected for this kind of compound exhibiting the out-of-plane bridging framework.[32,33]

The magnetic and structural data for [Cu(2pymehist)Cl](ClO$_4$) are consistent with the reduced number of exchange pathways involving mono-μ-chloro-bridged linear chain compounds of copper(II) already described in literature.[27c,34] Although there is a large body of data for chain compounds, there are few examples of both structural and magnetically characterised copper(II) chain complexes containing mono(μ-halo) bridges, and magneto-structural correlations in chains have not been developed in the same detail as those already carried out for dinuclear copper(II) systems.[32] Several authors have discussed the relevance of various geometrical aspects on the magnetic behaviour of chloride-bridged polynuclear copper(II) compounds. Hatfield has suggested that a smooth correlation exists between the exchange parameter J and the ratio θ/R (where θ is the magnitude of the angle at the Cu^{II}–Cl–Cu^{II} bridge and R is the longest Cu–Cl distance).[35] Table 1 shows the magnetic and structural parameters for some mono-μ-halogen–copper chains. The magnetic and structural data are consistent with the reduced number of exchange pathways but more data are required before the apparent magneto-structural correlation can be established. Following these correlations, overall ferromagnetic behaviour can be expected for values of the quotient θ/R lower than approximately 40 and higher than 57 while antiferromagnetic character appears when this quotient θ/R is between these two values as shown in Figure 3 (b).

Table 1. Structural and magnetic properties of some (μ-chloro)copper(II) compounds.[a][24,34]

Compound	R: Cu–Cl [Å]	Cu–Cl–Cu′ [°]	θ/R [°/Å]	J/k [cm^{-1}]
[Cu(dmso)$_2$Cl$_2$]	2.702(2)	144.6(1)	53.5	–6.1
[Cu(ImH)$_2$Cl$_2$]	2.751(6)	117.0	42.5	–2.1
[Cu(maep)Cl$_2$]	2.785(2)	113.58(5)	40.8	+1.58
[Cu(dipm)Cl$_2$]	2.6520(6)	144.60(2)	54.5	–3.2
[Cu(bpy)Cl$_2$]	2.674(3)	107.5(1)	40.2	–2.3
[Cu(caf)(H$_2$O)Cl$_2$]	2.788(2)	128.1	45.9	+0.48
[Cu(dpp)Cl$_4$]	2.5600(13)	98.46(4)	38.4	+6.0
[Cu(2pymehist)Cl](ClO$_4$)	2.614	118.0	45.1	–8.3

[a] Abbreviations: dmso = dimethyl sulfoxide, ImH = imidazole, bpy = 2,2′-bipyridine, maep = 2-[2-(methylamino)ethyl]pyridine, dpp = 2,3-di(2-pyridyl)pyrazine, caf = caffeine, dipm = bis(pyrimidin-2-yl)amine.

Characterisation of the Modified Electrode PVI/[Cu(2pymehist)Cl](ClO$_4$) Crosslinked with PEGDGE and Its Amperometric Response to H$_2$O$_2$

FT-Raman spectra of PVI, [Cu(2pymehist)Cl](ClO$_4$) and GC/PVI/[Cu(2pymehist)Cl](ClO$_4$) (see Figure 4, parts a–c) were recorded in order to confirm the presence of redox centres of the metal-organic redox hydrogel in the electrode surface. We think that the structure of the copper(II) complex on the electrode may be different from the X-ray determined structure of crystals of the compound. This is probably due to the Cu–Cl bond cleavage during the reaction of the PVI with the polynuclear copper(II) complex in aqueous solution, as confirmed by EPR analyses described previously. Each experimental spectrum was deconvoluted to a sum of Lorentzian curves. Figure 4 (d) shows the difference spectra for the experimental data and fitted spectra for GC/PVI-[Cu(2pymehist)Cl](ClO$_4$). Comparing the individual bands in the three samples enabled one inference about the presence of determined species in the electrode. Table 2 lists the frequencies and the corresponding assignments of the common bands observed in the GC/PVI/[Cu(2pymehist)Cl](ClO$_4$) electrode, PVI and in [Cu(2pymehist)Cl](ClO$_4$). Bands 1, 2 and 5 are characteristic out-of-plane vibrational modes of the PVI imidazole ring.[36] Bands 3 and 9 are pyridine C–H and CH$_3$ asymmetric vibrations of [Cu(2pymehist)Cl](ClO$_4$), respectively.[37] The remaining bands, ring vibration, black-body radiation, and C=N vibration were present in all cases.

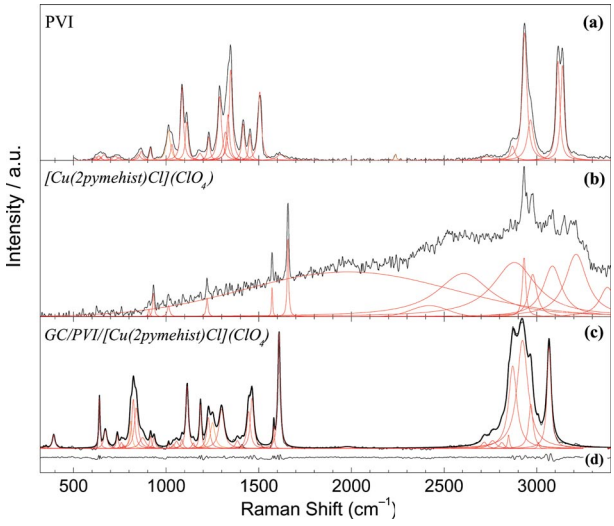

Figure 4. Raman spectra of PVI (a), [Cu(2pymehist)Cl](ClO$_4$) (b) and modified electrode GC/PVI/[Cu(2pymehist)Cl](ClO$_4$) (c). Red lines indicate the individual deconvoluted bands while the last curve in (d) shows the difference spectra among experimental and fitted spectra of (c).

Figure 5 shows the cyclic voltammograms of the modified electrode GC/PVI/[Cu(2pymehist)Cl](ClO$_4$), crosslinked with PEGDGE film, in a phosphate buffer at different scan rates. The cyclic voltammogram exhibits well-defined redox peaks at –0.20 and –0.35 V relative to the SCE which were assigned to the Cu^{II}/Cu^{I} redox process. The anodic peaks' currents are directly proportional to the square root of the scan rate in the range from 20 to 200 mV s^{-1}, as expected for a diffusion-controlled electron transfer process and they are shown in the insert of Fig-

Table 2. List of common Raman band frequencies [cm^{-1}] observed for the GC/PVI/[Cu(2pymehist)Cl](ClO_4) electrode, [Cu-(2pymehist)Cl](ClO_4) complex and PVI.[32,33]

	Electrode	Cu complex	PVI	Assignment
1	640	–	636	out-of-plane def. vibr. imidazole ring (4 H)
2	916	–	916	out-of-plane def. vib. imidazole ring (1 H)
3	935	932	–	C–H out of plane vibr. of pyridine
4	1013	1014	1012	ring vibr.
5	1185	–	1182	out-of-plane imidazole ring bending vib.
6	1228	1221	1229	C=N vibr.
7	1977	1975	1971	black-body radiation
8	2870	2868	2870	N–H stret. imidazole ring
9	2968	2967	–	CH_3 assym. vibr.

ure 5. Furthermore, the peak-to-peak separation increased with increasing scan rate due to the slow kinetics of electron transfer on the electrode surface.[38]

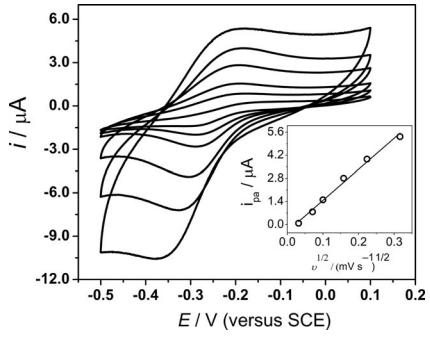

Figure 5. Cyclic voltammograms of an electrode modified with a crosslinked film of PVI-[Cu(2pymehist)Cl](ClO_4) in PBS (0.1 mol L^{-1}) at scan rates from 1 mV s^{-1} to 100 mV s^{-1}.

On the basis of the cyclic voltammetry results described above, we examined the performance characteristics of this electrode as an H_2O_2 sensor by using constant potential amperometry. The operating potential was stepped from –0.1 to –0.5 V in order to investigate the effect of the applied potential on the current response of the sensor, in a phosphate buffer solution (0.1 mol L^{-1}, pH 7.0), with different concentrations of hydrogen peroxide. As shown in Figure 6, the sensor response increases with decreasing potentials from –0.1 to –0.4 V, indicating that the sensor response is controlled both by the kinetics of the complex catalytic reaction and the electrochemical process. When the potential is more negative than –0.4 V, the response changes slightly, indicating that the sensor response is controlled by the diffusion of the substrate. Therefore, the potential of –0.4 V was selected as the optimum potential for the reduction of hydrogen peroxide. In this case, the sensor copper(II) complex-organic redox hydrogel plays the same role as the native catalase enzyme[7b,39] and a proposed mechanism is presented in Figure 7. This is based on the catalase mechanism and by considering that the copper complex [Cu(2pymehist)Cl](ClO_4) is dispersed in the PVI polymer, crosslinked with PEGDGE, in a way favourable to the formation of Cu^{I}-μ-O_2^{2-}–Cu^{I} sites. In a first step, the copper centres on the electrode surface are reduced to Cu^{I} when a potential of –0.4 V is applied to the modified working electrode, followed by the coordination of hydrogen peroxide to the copper ions. At the same time, the hydrogen peroxide might be reduced to water by oxidation of the copper centres and, consequently, giving signal amplification when the complex film is reduced at the electrode surface at –0.4 V. The reduction current observed is proportional to the hydrogen peroxide concentration which indicates that the immobilised polymer of the imine-copper(II) complex exhibits excellent electrocatalytic activity towards the reduction of H_2O_2. The same mechanism has also been reported for many amperometric biosensors based on the catalase enzymes.[7b,39]

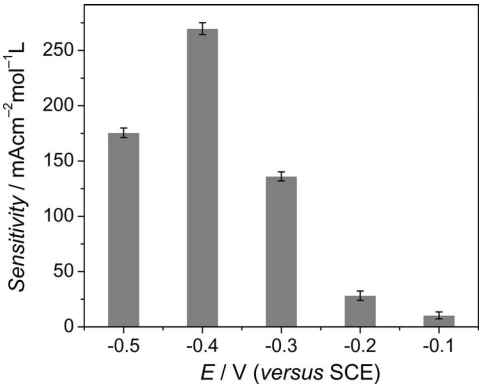

Figure 6. Effect of the applied potential on the sensitivity of the electrode modified with a crosslinked film of PVI/[Cu(2pymehist)-Cl](ClO_4), in 0.1 mol L^{-1} PBS (pH 7.0).

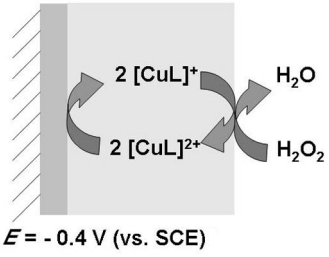

Figure 7. Scheme of the modified electrode with a crosslinked film of PVI/[Cu(2pymehist)Cl](ClO_4), in 0.1 mol L^{-1} PBS (pH 7.0).

Figure 8 shows the calibration curve of the GC/PVI/[Cu-(2pymehist)Cl](ClO_4) electrode as a sensor on addition of 12.5 μL mol L^{-1} H_2O_2 into a gently stirred air-saturated buffer solution. The electrode response time was less than 3 s. This fast response can be attributed to the direct electron transfer from the copper(II) complex-organic redox hydrogel to the electrode surface. When the concentration of H_2O_2 in the solution was too high, the electrode response time increased and the amperometric response became nonlinear. The insert in Figure 8 shows the calibration graph of H_2O_2 at the modified electrode. The calibration graph of current against H_2O_2 concentration is linear over the concentration range 1–30 mmol L^{-1} and the sensitivity is 268 mA mol^{-1} L cm^{-2} for H_2O_2 at –0.4 V relative to the SCE.

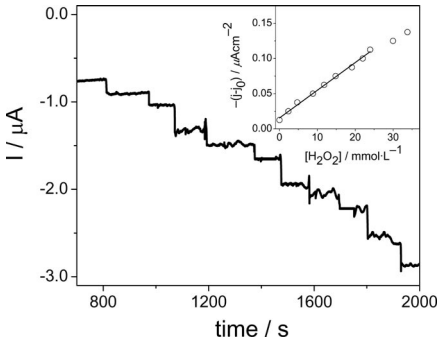

Figure 8. The response of electrode modified GC/PVI/[Cu(2pymehist)Cl](ClO_4) to H_2O_2, added in portions of 12.5 μmol L^{-1}. The electrode was operated at –0.4 V, in 0.1 mol L^{-1} PBS (pH 7.0).

Several methods have been used to construct a thin enzyme-film on the electrode surface to achieve and improve the direct electron transfer between native catalase enzyme and the electrode surface. This is because it is difficult for catalase to exchange electrons with the electrode surface directly since its redox centre, the haeme group, is deeply buried in its peptide chains.[40] In particular, direct electrochemistry of catalase on multi-walled carbon nanotubes (MWCNT) has been observed at –0.50 V relative to the SCE in 0.1 mol L^{-1} Tris-HCl buffer solution (pH 7.0), while there is no electrochemical response of catalase on a bare GC electrode.[41] In this work, a similar potential was observed for the GC/PVI/ [Cu(2pymehist)Cl](ClO_4) electrode, the latter having good sensitivity for detection of hydrogen peroxide indicating that the [Cu(2pymehist)Cl](ClO_4) complex is mimicking the catalase active site. This redox hydrogel-based sensor showed a wide linear response range for H_2O_2 detection when compared with native catalase enzyme immobilized in multi-walled carbon nanotubes on a gold surface electrode (1–5 mmol L^{-1}).[41] The detection limit for this biomimetic material was found to be 4×10^{-6} mol L^{-1}, using the ratio of three for the lowest standard deviation of the background current. Further studies showed that this modified electrode is very stable. When it was stored in a pH 7.0 PBS for at least two weeks at 4 °C, the electrode retained more than 90% of its initial response to the reduction of H_2O_2.

Conclusions

A new mono-μ-chloro-bridged imine-copper(II) compound was synthesised and characterised. The determined crystal structure of this compound exhibited uniform chains formed by stacking of parallel pyramidal units with the uncoordinated perchlorate ions located between the layers to balance the charge. The magnetic measurements on this compound show different types of interactions, reflecting the ligand bridging modes and the geometric parameters. The corresponding variation of the magnetic susceptibility with temperature shows a maximum around 9.4 K, indicating an intramolecular magnetic coupling between the copper centres [J/k = (–12.3 ± 0.2) K] and further interactions between adjacent chains [$J'z/k$ = –(10.4 ± 1.7) K] should be taken into account. Therefore, a linear Curie–Weiss analysis at temperatures far above the typical coupling constants indicated that the overall interaction is antiferromagnetic (Θ_{CW} = –14 K). Furthermore, this new inorganic-organic zigzag polymer was linked covalently to PVI, on a vitreous carbon electrode surface and used as biomimetic material for the efficient analytical determination of hydrogen peroxide. In this case, the sensitivity obtained was 268 mA mol^{-1} L cm^{-2} at –0.4 V relative to the SCE in phosphate buffer solution (pH 7.0). A wide linear range from 1 to 30 mmol L^{-1} for hydrogen peroxide detection was observed. These results suggest that the composite film formed by a modified electrode GC/PVI/[Cu(2pymehist)Cl](ClO_4), crosslinked with PEGDGE, is a promising material for potential applications as an enzyme-free biosensor for catalase-like activity.

Experimental Section

Materials and Physical Measurements: All reagents were of analytical grade, purchased from different sources, and used without further purification. The following abbreviations were used: 2pymehist = 2-(4-imidazolyl)ethylimino-6-methylpyridine, is a diimine ligand derived from condensation of 6-methyl-2-carboxypyridine with histamine dihydrochloride. The PVI polymer was prepared by Dr. Heller's group by using a method that was already reported in a previous publication.[42]

Elemental analyses were performed using a Perkin–Elmer 2400 CHN elemental analyser. Optical absorbance spectra were recorded on a Shimadzu UV-1601PC spectrophotometer. EPR spectra were acquired with a Bruker EMX instrument, operating at the X-band frequency (9.35 GHz), using standard Wilmad quartz tubes, at 77 K. Conductivity experiments with the complexes studied (in 1 mmol dm^{-3} aqueous solution) were carried out on a Digimed DM-31 instrument, using a 10.0 mmol dm^{-3} KCl solution as standard (specific conductivity = 1412.0 μS cm^{-1}, at 25 °C). An FT-Raman spectrometer (Bruker RFS 100/S; Bruker Optics GmbH, Ettlingen, Germany) was used with a Nd:YAG laser at 1064 nm as the excitation light source. The laser power at the sample was maintained at 30 mW while the resolution was set to 4 cm^{-1}. The spectra were recorded using 100 scans (nearly 3 min of acquisition time). The temperature dependence of the magnetic susceptibility of polycrystalline samples was measured between 1.8 and 290 K, at a field of 500 Oe, using a computer-controlled SQUID magnetometer. Diamagnetic correlations were made using Pascal's constants. Cyclic voltammetry (CV) and chronoamperometry (CA) experiments were performed with an Autolab PGSTAT30 (Eco Chemie) electrochemical system. All potentials are referred to the saturated calomel electrode (SCE) while a platinum foil was employed as the auxiliary electrode. As the working electrode, a glassy carbon electrode (3 mm diameter) was used. Before experiments, the buffer solution was bubbled with pure nitrogen for a thoroughly anaerobic situation. All measurements were performed at room temperature.

Synthesis of [Cu(2pymehist)Cl](ClO_4): Histamine dihydrochloride (1.840 g, 10 mmol) was added to a solution of 6-methylpyridine-2-carboxylic acid (1.249 g, 10 mmol) in water (40 mL) and the mixture was stirred at room temperature for 40 min. A water solution (10 mL) of [$Cu(ClO_4)_2$]·$6H_2O$ (3.705 g, 10 mmol) was then added

at once. After 48 h of standing, a green crystalline precipitate was observed which was collected by filtration, washed with small amounts of cooled methanol and diethyl ether and finally dried in vacuo over P_2O_5. The obtained yield was 73%. $C_{12}H_{14}ClCuN_4(ClO_4)$: calcd. C 34.92, H 3.42, N 13.57; found: C 34.30, H 3.40, N 13.02. Λ_{Cu} = 71.07 S cm^2 mol^{-1} in methanol. UV/Vis (methanol): λ_{max} (ε, L mol^{-1} cm^{-1}) = 203 (22.8×10^3), 299 (8.58×10^3), 744 (135) nm.

Preparation of the Hybrid Material PVI/[Cu(2pymehist)Cl](ClO$_4$): Preparation of the hybrid material was carried out according to previously published procedures[42] with suitable modifications. [Cu(2pymehist)Cl](ClO_4) (100 mg) and PVI (80 mg, 1:5 molar ratio) in absolute ethanol (100 mL) were heated to reflux for 3 d. The solvent was evaporated and the product was redissolved in ethanol/water (30:70 v/v) containing NaCl (50 mmol L^{-1}) and HEPES (10 mmol L^{-1}). The solution was passed through a Sephadex G-25 size exclusion column. The high molar mass polymer was collected and partially methylated by adding CH_3I (4 mg) to the polymer (15 mg) dissolved in ethylene glycol (0.5 mL) and DMF (0.5 mL). The solution was stirred for 24 h at room temperature. Bio-Rad AG 1-X8 ion exchange beads were added and the total volume was brought to 10 mL with water and stirred for 16 h at room temperature. The beads were removed by filtering and the solution was dialysed against water for 2 d. The solution was then evaporated and the polymer collected.

Preparation of the Hybrid Film Modified GC Electrode and Chronoamperometry Studies Towards H_2O_2 Detection: Vitreous carbon electrodes (3 mm diameter) were used. These were polished and cleaned using three grades of alumina slurry (5, 1, 0.3 μm) with sonication and rinsing between grades. They were tested in a phosphate buffer by scanning between the potentials of interest (–0.5 to 0.5 V relative to the SCE) to ensure that the electrochemistry was featureless. Films were prepared by adding PVI/[Cu(2pymehist)Cl](ClO_4) (2 μL, 20 mg mL^{-1}) and the crosslinker PEGDGE (1 μL, 5.6 mg mL^{-1}), followed by mixing of these solutions on the electrode surface with the tip of a syringe. The electrodes were then placed in an evacuated desiccator for 16 h prior to use.

After its preparation, the modified electrode was washed and used as an amperometric sensor in a phosphate buffer 0.1 mol L^{-1} (pH 7.0). Amperometric measurements were carried out in a stirred cell by applying a potential of –0.5 V, relative to the SCE, to the working electrode.

X-ray Crystallographic Procedures: A single crystal of [Cu(2pymehist)Cl](ClO_4) was mounted on the Enraf–Nonius CAD4 diffractometer at room temperature and, using 25 automatically centred reflections (θ from 11.66 to 18.25°), the cell parameters were obtained and refined. Table 3 shows the data collection and the refinement conditions. The data were corrected by absorption factors [μ(Mo-K_α) = 1.656 mm^{-1}] using the PSISCAN method.[43] The structure was solved using the WingX software package[44] incorporating SHELXS-97 and refined by means of least-squares procedures on a F^2 with the aid of the program SHELXL97.[45] The hydrogen atoms were located in their ideal positions and not refined, except those for the water molecule that were located in a difference Fourier map. All non-hydrogen atoms were refined anisotropically. Drawings of molecules were performed with the program ORTEP-3.[46] The structural analysis was performed with the PLATON system.[47]

Although several crystals of [Cu(2pymehist)Cl](ClO_4) were selected for the data collection, their poor quality precluded the obtaining of a good refinement. In addition, the structure shows disorder of the solvent perchlorate ion and the refined site occupancy factor of the water molecule was 0.33.

Table 3. Crystal data and structural parameters for the complex [Cu(2pymehist)Cl](ClO_4).

Formula	$[CuClN_4C_{12}H_{14}]ClO_4(H_2O)$
Formula weight	418.67
Crystal system	monoclinic
Space group	$P2_1/a$
a [Å]	7.677(1)
b [Å]	15.528(2)
c [Å]	14.045(2)
[°]	96.22(1)
V [Å^3]	1664.5(4)
Z	4
D_{calc} [g cm^{-3}]	1.671
Mo-K_α [mm^{-1}]	1.656
F(000)	849
Crystal size [mm]	$0.05\times0.10\times0.30$
T [K]	291(2)
λ Mo-K_α [Å]	0.71073
θ min./max. [°]	2.6–28.5
Index ranges	0:10; 0:20; $\bar{1}\bar{8}$:18
Total, unique data, R_{int}	4539, 4234, 0.078
Observed data [$I > 2.0\ \sigma(I)$]	1447
N_{ref}, N_{par}	4234, 219
R, wR_2, S	0.062, 0.277, 0.92
$w = 1/[\sigma^2(F_o^2) + (0.0879P)^2]$	$P = (F_o^2 + 2F_c^2)/3$
min, max. residual electron density [e Å^{-3}]	–0.53, 0.53

CCDC-710681 contains the supplementary crystallographic data for this paper. These data can be obtained free of charge from The Cambridge Crystallographic Data Centre via www.ccdc.cam.ac.uk/data_request/cif.

Supporting Information (see also the footnote on the first page of this article): Selected bond lengths, angles and hydrogen bonds to the determined crystal structure [Cu(2pymehist)Cl](ClO_4) are listed in Tables S1, S2 and S3.

Acknowledgments

Financial support from the Brazilian agencies Fundação de Amparo à Pesquisa do Estado de São Paulo (FAPESP), Grant No. 05/60596-8 and 07/50968-0, and Conselho Nacional de Desenvolvimento Científico e Tecnológico (CNPq), Grant No. 555592/2006-5 and 301018/2006-5, is gratefully acknowledged. P. M. T. also thanks FAPESP for fellowship (08/51074-6). The authors thank Dr. Airton A. Martin, from Universidade do Vale do Paraíba/Brazil for the use of Raman instrumentation. W. A. A. is grateful to Professor Adam Heller, from the Department of Chemical Engineering, University of Texas at Austin, USA, for samples of PVI.

[1] a) A. B. Descalzo, R. Martinez-Manez, R. Sancenon, K. Hoffmann, K. Rurack, *Angew. Chem. Int. Ed.* **2006**, *45*, 5924–5948; b) M. A. Reed, C. Zhou, C. J. Muller, T. P. Burgin, J. M. Tour, *Science* **1997**, *278*, 252–254.

[2] a) H. Nagasaka, M. Watanabe, *Synth. Met.* **1995**, *69*, 557–558; b) N. Mano, V. Soukharev, A. Heller, *J. Phys. Chem. B* **2006**, *110*, 11180–11187; c) Y. C. Weng, F.-R. F. Fan, A. J. Bard, *J. Am. Chem. Soc.* **2005**, *127*, 17576–17577; d) P. A. Fiorito, S. I. Córdoba de Torresi, *J. Electroanal. Chem.* **2005**, *581*, 31–37; e) W. A. Alves, V. Pfaffen, P. I. Ortiz, S. I. C. de Torresi, R. M. Torresi, *J. Braz. Chem. Soc.* **2008**, *19*, 651–659.

[3] a) H.-H. Kim, N. Mano, Y. Zhang, A. Heller, *J. Electrochem. Soc.* **2003**, *150*, A209-A213; b) E. Katz, I. Willner, *J. Am. Chem. Soc.* **2003**, *125*, 6803–6813; c) A. Heller, B. Feldman, *Chem. Rev.* **2008**, *108*, 2482–2505; d) S. D. Minteer, B. Y. Liaw, M. J. Cooney, *Curr. Opin. Biotechnol.* **2007**, *18*, 228–234; e) A. Heller, *Curr. Opin. Chem. Biol.* **2006**, *10*, 664–672; f) S. C. Barton, J. Gallaway, P. Atanassov, *Chem. Rev.* **2004**, *104*, 4867–4886

[4] a) V. R. Goncales, R. P. Salvador, M. R. Alcantara, S. I. Córdoba de Torresi, *J. Electrochem. Soc.* **2008**, *155*, K140–K145; b) W. A. Alves, P. A. Fiorito, S. I. Córdoba de Torresi, R. M. Torresi, *Biosen. Bioelectron.* **2006**, *22*, 298–305; c) E. S. Forzani, M. Otero, M. A. Pérez, M. L. Teijelo, E. J. Calvo, *Langmuir* **2002**, *18*, 4020–4029; d) W. A. Alves, P. A. Fiorito, G. Froyer, F. E. Haber, L. Vellutini, R. M. Torresi, S. I. C. de Torresi, *J. Nanosci. Nanotechnol.* **2008**, *8*, 3570–3576.

[5] a) J. Kim, H. Jia, P. Wang, *Biotechnol. Adv.* **2006**, *24*, 296–308; b) C. M. Moore, N. L. Akers, A. D. Hill, Z. C. Johnson, S. D. Minteer, *Biomacromolecules* **2004**, *5*, 1241–1247; c) N. L. Akers, C. M. Moore, S. D. Minteer, *Electrochim. Acta* **2005**, *50*, 2521–2525.

[6] a) M. D. P. T. Sotomayor, A. A. Tanaka, L. T. Kubota, *J. Electroanal. Chem.* **2002**, *536*, 71–81; b) Y. Hasebe, T. Gu, *J. Electroanal. Chem.* **2005**, *576*, 177–181; c) Y. Hasebe, T. Akiyama, T. Yagisawa, S. Uchiyama, *Talanta* **1998**, *47*, 1139–1147; d) M. D. P. T. Sotomayor, A. A. Tanaka, L. T. Kubota, *Electrochim. Acta* **2003**, *48*, 855–865.

[7] a) M. Zamocky, F. Koller, *Prog. Biophys. Mol. Biol.* **1999**, *72*, 19–66; b) X. Chen, H. Xie, J. Kong, J. Deng, *Biosens. Bioelectron.* **2001**, *16*, 115–120; c) I. Fridovich, *Annu. Rev. Biochem.* **1995**, *64*, 97–112.

[8] a) M. Janotta, F. Vogt, H. S. Voraberger, W. Waldhauser, J. M. Lackner, C. Stotter, M. Beutl, B. Mizaikoff, *Anal. Chem.* **2004**, *76*, 384–391; b) X. S. Chai, Q. X. Hou, Q. Luo, J. Y. Zhu, *Anal. Chim. Acta* **2004**, *507*, 281–284; c) C. Matsubara, N. Kawamoto, K. Takamura, *Analyst* **1992**, *117*, 1781–1784; d) S. Hanaoka, J. Lin, M. Yamada, *Anal. Chim. Acta* **2001**, *426*, 57–64.

[9] a) J. Gong, L. Wang, K. Zhao, D. Song, *Electrochem. Commun.* **2008**, *10*, 123–126; b) S. Q. Liu, Z. H. Dai, H. Y. Chen, H. X. Ju, *Biosens. Bioelectron.* **2004**, *19*, 963–969; c) M. R. Guascito, E. Filippo, C. Malitesta, D. Manno, A. Serra, A. Turco, *Biosens. Bioelectron.* **2008**, *24*, 1057–1063; d) A. S. Santos, N. Durán, L. T. Kubota, *Electroanalysis* **2005**, *17*, 1103–1111; e) H.-J. Jiang, H. Yang, D. L. Akins, *J. Electroanal. Chem.* **2008**, *623*, 181–186.

[10] a) T. Tatsuma, T. Watanabe, *Anal. Chem.* **1991**, *63*, 1580–1585; b) F. W. Scheller, U. Wollenberger, C. Lei, W. Jin, B. Ge, C. Lehmann, F. Lisdat, V. Fridman, *Rev. Molecul. Biotechnol.* **2002**, *82*, 411–424; c) W. Huang, J. Jia, Z. Zhang, X. Han, J. Tang, J. Wang, S. Dong, E. Wang, *Biosens. Bioelectron.* **2003**, *18*, 1225–1230; d) C. Camacho, J. C. Matias, D. Garcia, B. K. Simpson, R. Villalonga, *Electrochem. Commun.* **2007**, *9*, 1655–1660; e) T. Gu, Y. Hasebe, *Anal. Chim. Acta* **2004**, *525*, 191–198.

[11] a) A. A. Karyakin, O. V. Gitelmacher, E. E. Karyakina, *Anal. Chem.* **1995**, *67*, 2419–2423; b) A. A. Karyakin, E. E. Karyakina, L. Gorton, *Talanta* **1996**, *43*, 1597–1606; c) A. A. Karyakin, E. F. Karyakina, L. Gorton, *J. Electroanal. Chem.* **1998**, *456*, 97–104; d) A. A. Karyakin, E. A. Kotel'nikova, L. V. Lukachova, E. E. Karyakina, J. Wang, *Anal. Chem.* **2002**, *74*, 1597–1603; e) P. A. Fiorito, S. I. Córdoba de Torresi, *Talanta* **2004**, *62*, 649–654; f) F. Ricci, G. Palleschi, *Biosen. Bioelectron.* **2005**, *21*, 389–407; g) D. Moscone, D. D'Ottavi, D. Compagnone, G. Palleschi, A. Amine, *Anal. Chem.* **2001**, *73*, 2529–2535.

[12] a) E. Bustos, J. Manriquez, G. Orozco, L. A. Godinez, *Langmuir* **2005**, *21*, 3013–3021; b) S. G. Wu, T. L. Wang, C. Q. Wang, Z. Y. Gao, C. Q. Wang, *Electroanalysis* **2007**, *19*, 659–667; c) S. Wu, H. T. Zhao, H. X. Ju, C. G. Shi, J. W. Zhao, *Electrochem. Commun.* **2006**, *8*, 1197–1203; d) Y. Liu, L. M. Hu, S. Q. Yang, *Microchim. Acta* **2008**, *160*, 357–365.

[13] a) G. D. Storrier, K. Takada, H. D. Abruña, *Langmuir* **1999**, *15*, 872–884; b) W. Mori, S. Takamizawa, C. N. Kato, T. Ohmura, T. Sato, *Microporous Mesoporous Mater.* **2004**, *73*, 31–46; c) L. K. Thompson, *Coord. Chem. Rev.* **2002**, *233*, 193–206.

[14] a) P. H. Dinolfo, J. T. Hupp, *Chem. Mater.* **2001**, *13*, 3113–3125; b) G. F. Swiegers, T. J. Malefetse, *Chem. Rev.* **2000**, *100*, 3483–3537; c) O. Kahn, *Acc. Chem. Res.* **2000**, *33*, 647–657; d) O. M. Yaghi, H. Li, C. Davis, D. Richardson, T. L. Groy, *Acc. Chem. Res.* **1998**, *31*, 474–484; e) J.-M. Lehn, *Supramolecular Chemistry: Concepts and Perspectives*, VCH, Weinheim, **1995**.

[15] a) L.-G. Qiu, A.-J. Xie, L.-D. Zhang, *Adv. Mater.* **2005**, *17*, 689–692; b) W. Mori, T. Sato, T. Ohmura, C. N. Kato, T. Takei, *J. Solid State Chem.* **2005**, *178*, 2555–2573.

[16] a) Y. Sunatsuki, Y. Motoda, N. Matsumoto, *Coord. Chem. Rev.* **2002**, *226*, 199–209; b) J. A. R. Navarro, B. Lippert, *Coord. Chem. Rev.* **2001**, *222*, 219–250; c) J. M. Dominguez-Vera, F. Camara, J. M. Moreno, E. Colacio, H. Stoeckli-Evans, *Inorg. Chem.* **1998**, *37*, 3046–3050.

[17] a) W. A. Alves, G. Cerchiaro, A. Paduan-Filho, D. M. Tomazela, M. N. Eberlin, A. M. D. C. Ferreira, *Inorg. Chim. Acta* **2005**, *358*, 3581–3591; b) W. A. Alves, S. A. de Almeida-Filho, R. H. A. Santos, A. M. D. C. Ferreira, *Inorg. Chem. Commun.* **2003**, *6*, 294–299; c) W. A. Alves, S. A. de Almeida-Filho, M. V. Almeida, A. Paduan-Filho, C. C. Becerra, A. M. D. C. Ferreira, *J. Mol. Catal. A* **2003**, *198*, 63–75; d) W. A. Alves, M. A. D. Azzellini, R. E. Bruns, A. M. D. C. Ferreira, *Int. J. Chem. Kin.* **2001**, *33*, 472–479.

[18] M. A. Bizeto, W. A. Alves, C. A. S. Barbosa, A. M. D. C. Ferreira, V. R. L. Constantino, *Inorg. Chem.* **2006**, *45*, 6214–6221.

[19] Matsumoto, *Angew. Chem. Int. Ed. Engl.* **1997**, *36*, 1860.

[20] W. A. Alves, S. A. Almeida-Filho, R. H. A. Santos, A. Paduan-Filho, A. M. D. C. Ferreira, *J. Braz. Chem. Soc.* **2004**, *15*, 872–883.

[21] A. W. Addison, T. N. Rao, J. Reedijk, J. V. Rijn, G. C. Verschoor, *J. Chem. Soc., Dalton Trans.* **1984**, 1349–1356.

[22] B. K. S. Lundberg, *Acta Chem. Scand.* **1972**, *26*, 3977–3983.

[23] a) L. Pauling, *The Nature of the Chemical Bond*, Cornell University Press, Ithaca, NY, **1960**; b) A. M. Pendás, A. Costales, V. Luaña, *J. Phys. Chem. B* **1998**, *102*, 6937–6948.

[24] G. A. van Albada, O. Roubeau, P. Gamez, H. Kooijman, A. L. Spek, J. Reedijk, *Inorg. Chim. Acta* **2004**, *357*, 4522–4527.

[25] A. Bernalte-Garcia, F. J. Garcia-Barros, F. J. Higes-Rolando, F. Luna-Giles, R. Pedrero-Marin, *J. Inorg. Biochem.* **2004**, *98*, 15–23.

[26] K. T. McGregor, Z. G. Soos, *Inorg. Chem.* **1976**, *15*, 2159–2165.

[27] a) S. S. Eaton, G. R. Eaton, *J. Am. Chem. Soc.* **1982**, *104*, 5002–5003; b) S. S. Eaton, K. M. More, B. M. Sawant, G. R. Eaton, *J. Am. Chem. Soc.* **1983**, *105*, 6560–6567; c) R. Cortés, L. Lezama, I. Ruiz de Larramendi, G. Madariaga, J. L. Mesa, F. J. Zuñiga, T. Rojo, *Inorg. Chem.* **1995**, *34*, 778–786.

[28] W. A. Alves, I. A. Bagatin, A. M. D. C. Ferreira, *Inorg. Chim. Acta* **2001**, *321*, 11–21.

[29] W. E. Estes, D. P. Gavel, W. E. Hatfield, D. J. Hodgson, *Inorg. Chem.* **1978**, *17*, 1415–1421.

[30] J. C. Bonner, M. E. Fisher, *Phys. Rev. A* **1964**, *135*, 640.

[31] a) E. Ruiz, P. Alemany, S. Alvarez, J. Cano, *J. Am. Chem. Soc.* **1997**, *119*, 1297–1303; b) W. A. Alves, R. H. A. Santos, A. Paduan-Filho, C. C. Becerra, A. C. Borin, A. M. D. C. Ferreira, *Inorg. Chim. Acta* **2004**, *357*, 2269–2278.

[32] P. Alemany, S. Alvarez, *Chem. Mater.* **1990**, *2*, 723–728.

[33] O. Kahn, *Molecular Magnetism*, VCH, Weinheim, **1993**.

[34] F. J. Barros-García, A. Bernalte-García, F. J. Higes-Rolando, F. Luna-Giles, A. M. Pizarro-Galán, E. Viñuelas-Zahínos, *Z. Anorg. Allg. Chem.* **2005**, *631*, 1898–1902.

[35] W. E. Hatfield, *Comments, Inorg. Chem.* **1981**, *1*, 105–121.

[36] a) I. Ashikawa, K. Itoh, *Biopolymers* **1979**, *18*, 1859–1876; b) D. A. Carter, J. E. Pemberton, *J. Raman Spectrosc.* **1997**, *28*,

939–946; c) S. Dong, T. G. Spiro, *J. Am. Chem. Soc.* **1998**, *120*, 10434–10440; d) H. Baranska, J. Kuduk-Jaworska, *J. Raman Spectrosc.* **1997**, *28*, 1–7.

[37] A. C. Sant'Ana, W. A. Alves, R. H. A. Santos, A. M. D. C. Ferreira, M. L. A. Temperini, *Polyhedron* **2003**, *22*, 1673–1682.

[38] a) E. Laviron, *J. Electroanal. Chem.* **1979**, *101*, 19–28; b) E. Laviron, *J. Electroanal. Chem.* **1974**, *52*, 355–393.

[39] a) L. Wang, J. Wang, F. Zhou, *Electroanalysis* **2004**, *16*, 627–632; b) Z. Zhang, S. Chouchane, R. S. Magliozzo, J. F. Rusling, *Chem. Commun.* **2001**, 177–178.

[40] a) J. W. Di, M. Zhang, K. A. Yao, S. P. Bi, *Biosens. Bioelectron.* **2006**, *22*, 247–252; b) A. M. Yu, F. Caruso, *Anal. Chem.* **2003**, *75*, 3031–3037; c) Z. Zhang, S. Chouchane, R. S. Magliozzo, J. F. Rusling, *Anal. Chem.* **2002**, *74*, 163–170.

[41] H. Zhou, T.-H. Lu, H.-X. Shi, Z.-H. Dai, X.-H. Huang, *J. Electroanal. Chem.* **2008**, *612*, 173–178.

[42] C. Taylor, G. Kenausis, I. Katakis, A. Heller, *J. Electroanal. Chem.* **1995**, *396*, 511–515.

[43] A. C. T. North, D. C. Phillips, F. S. Mathews, *Acta Crystallogr., Sect. A* **1968**, *24*, 351.

[44] L. J. Farrugia, *J. Appl. Crystallogr.* **1999**, *32*, 837–838.

[45] SHELXS97, SHELXL97: G. M. Sheldrick, Programs for Crystal Structure Analysis, rel. 97-2, University of Göttingen, Germany, **1997**.

[46] L. J. Farrugia, *J. Appl. Crystallogr.* **1997**, *30*, 565.

[47] A. L. Speck, PLATON: A Multipurpose Crystallographic Tool, Utrecht University, The Netherlands, **1998**.

Received: December 17, 2008
Published Online: April 14, 2009

